ELSEVIER

CrossMark

Unification of soil feedback patterns under different evaporation conditions to improve soil differentiation over flat area

Shanxin Guo [a,b], A-Xing Zhu [c,d,e,f,g,*], Lingkui Meng [b], James E. Burt [g], Fei Du [g], Jing Liu [g], Guiming Zhang [g]

[a] Shenzhen Institutes of Advanced Technology, Chinese Academy of Sciences, Shenzhen 518055, PR China
[b] School of Remote sensing and Information Engineering, Wuhan University, Wuhan 430079, PR China
[c] Key Laboratory of Virtual Geographic Environment (Nanjing Normal University), Ministry of Education, Nanjing 210023, PR China
[d] State Key Laboratory Cultivation Base of Geographical Environment Evolution (Jiangsu Province), Nanjing 210023, PR China
[e] Jiangsu Center for Collaborative Innovation in Geographical Information Resource Development and Application, Nanjing 210023, PR China
[f] State key Laboratory of Resources and Environmental Information System, Institute of Geographical Sciences and Natural Resources Research, Chinese Academy of Sciences, Beijing 100101, PR China
[g] Department of Geography, University of Wisconsin-Madison, Madison, Wisconsin 53706, USA

ARTICLE INFO

ABSTRACT

Detailed and accurate information on the spatial variation of soil types and soil properties are critical components of environmental research and hydrological modeling. Early studies introduced a soil feedback pattern as a promising environmental covariate to predict spatial variation over low-relief areas. However, in practice, local evaporation can have a significant influence on these patterns, making them incomparable at different locations. This study aims to solve this problem by examining the concept of transforming the dynamic patterns of soil feedback from the original time-related space to a new evaporation-related space. A study area in northeastern Illinois with large low-relief farmland was selected to examine the effectiveness of this idea. Images from MODIS in Terra for every April–May period over 12 years (2000–2011) were used to extract the soil feedback patterns. Compared to the original time-related space, the results indicate that the patterns in the new evaporation-related space tend to be more stable and more easily captured from multiple rain events regardless of local evaporation conditions. Random samples selected for soil subgroups from the SSURGO soil map show that patterns in the new space reveal a difference between different soil types. And these differences in patterns are closely related to the difference in the soil structure of the surface layer.

1. Introduction

The soil-landscape model is based on the state equation of soil formation (Jenny, 1941), which assumes that the development of soil is determined by environmental conditions including climate, parent material, topography, biology and time. Using this concept, it is possible to predict the spatial variation of soil properties and soil types from the spatial variation of environmental conditions (covariates). Many studies succeed to predict soil types or soil properties in strong heterogeneous soil-landscapes, such as mountain area (McKenzie and Ryan, 1999; Zhu, 1997; Zhu et al., 2010b). Over

low-relief areas like plains and most farmland, however, commonly used environmental covariates, such as elevation, slope gradient and vegetation, often fail to effectively indicate the spatial variation of soil types and properties (Iqbal et al., 2005; Zhu et al., 2010a).

To overcome the difficulty of soil mapping in low-relief areas, some attempts have been made to predict the variation of soil using multispectral remote sensing (Coleman et al., 1993; Odeh and Mcbratney, 2000; Sullivan et al., 2005). Hyperspectral remote sensing data with narrow bandwidths and high spectral resolution are also used to capture soil surface characteristics (Gomez et al., 2008; Lagacherie et al., 2008). However, in most studies, soil surface characteristics, such as soil texture and soil surface roughness, are generally obtained based on only one or a few images captured by multispectral or hyperspectral sensors at one or a few specific times. In fact, soil reflectance varies during the soil drying process, which is closely related to both soil properties and soil surface water content (Lobell and Asner, 2002; Muller and Decamps,

2001; Philpot, 2010; Wang and Qu, 2009; Weidong et al., 2002). As a result, the accuracy of the prediction may be highly related to sensor noise, atmospheric conditions and the soil surface texture conditions at that specific time (Anderson and Croft, 2009; Mulder et al., 2011).

The soil feedback pattern was introduced as a new environmental covariate to effectively indicate the spatial variation of soil types and soil properties over low relief areas (Liu et al., 2012; Zhu et al., 2010a). Instead of collecting soil information at one or a few specific times, soil feedback pattern records the whole reflectance changes during soil drying process. The original definition for the feedback pattern is organized as three dimensional, which is time related and arranged with time as the X axis, wavelength as the Y axis, and soil surface reflectance as the Z axis(Zhu et al., 2010a). As shown in Fig. 1a, after a rain event, the daily surface reflectance of soil was immediately captured by the MODIS sensor for a short time period (5–7 days) and organized in this three-dimensional space. Conceptually, the rainfall is seen as an input, and the pattern is seen as the soil feedback response to the rainfall. So this pattern can also be seen as "the soil surface reflectance pattern" in response to the soil moisture changes during the soil drying process. The basic assumption of soil feedback pattern is similar soil with similar type or similar hydrological properties will have similar behavior during the soil drying from moisture saturated condition to air-dry condition. The different soils will show different drying behavior. Previous study shows the soil feedback pattern can be used to indicate the soil types and soil properties and the pattern variations at different locations are indicative of the variation in soil types at those locations (Liu et al., 2012; Zhu et al., 2010a).

The feedback patterns representing the soil drying process, however, are highly influenced by local evaporation conditions, which are related to fluctuations in local air temperature, humidity and wind speed. This phenomenon causes two problems when comparing the patterns at different locations: first, the difference between patterns over a large area is not just related to the difference in soils, but also to the difference in evaporation conditions. This makes it hard to tell whether the differences can be attributed to differences in soil or evaporation conditions. Second, at a given location, different rain events could create considerably different patterns due to the evaporation variation. In other words, patterns observed at a given location but at different times cannot be compared. In order to predict the spatial variation of soil over large areas, it is necessary to solve these two problems so that the patterns, even with different evaporation conditions, are comparable. The objective of this study is to find a way to solve these incomparable problems to make patterns from different evaporation conditions comparable.

In this study, we present an improved space for measuring the soil feedback patterns in an effort to solve this problem. The improved space is referred to as the evaporation-related space, which includes local evaporation conditions as a component. In this new space, soils with similar properties tend to present the same pattern regardless of local evaporation conditions. This makes patterns under different evaporation conditions comparable. This approach was applied in a large area of farmland in northeastern Illinois, in the United States, as a case study. The major objectives of the study are as follows:

- Describe a new space that allows soil surface reflectance patterns after rainfall to represent soil characteristics regardless of different evaporation conditions.
- Overcome the limitation that requires the original soil feedback pattern be observed in the same rain event with similar evaporation conditions before patterns can be compared. The pattern in the new space can be observed from multiple rain events, which makes the data collection of soil feedback patterns easier in practice.
- Provide a potential application that uses the soil feedback pattern to predict spatial variation in soil over a large area by solving two key problems that make the comparison of patterns in the original space across different evaporation conditions impossible.

2. Methodology

2.1. Basic idea

After a rainfall, the initial saturated water content of the top layer of the same soil will be nearly uniform and is highly related to the soil's surface texture, surface structure and hydrological properties(Lal and Shukla, 2004). During the soil drying process, soil evaporation is the primary cause of water loss in the soil surface layer (Mellouli et al., 2000). Therefore, the water content in the top layer of soil (1–5 cm deep) will have a similar value at every step of soil evaporation if the soils are alike. Previous studies have shown that the same soils with the same surface water content will have similar reflectance curves in the electromagnetic spectrum (Lobell and Asner, 2002; Muller and Decamps, 2001; Somers et al., 2010). As a result, soil surface reflectance during the soil drying process
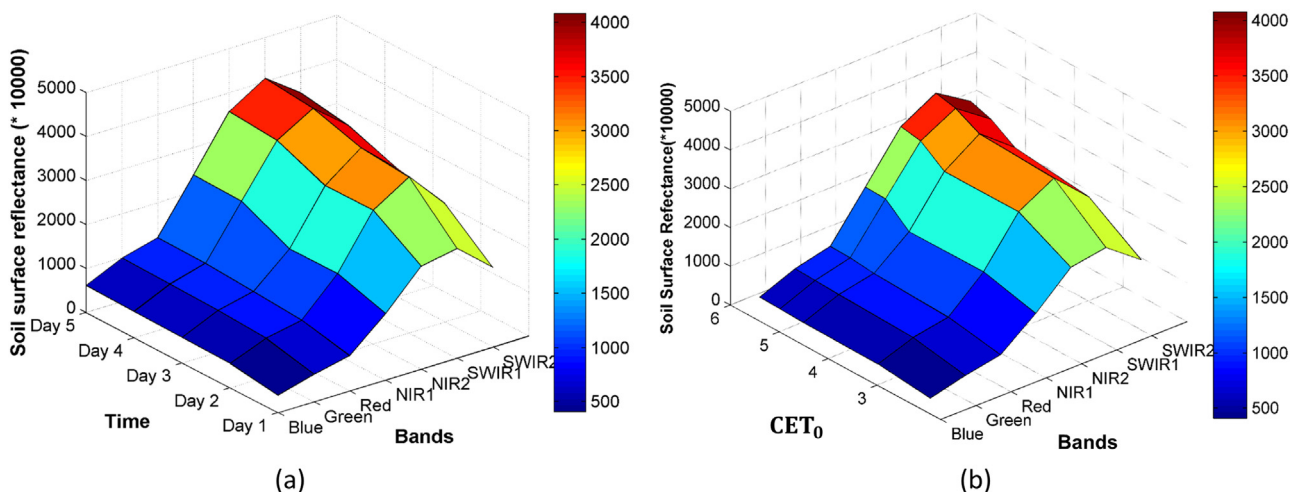

Fig. 1. Illustration of soil reflectance change after one rain event in two spaces at a given location. (a) pattern in the time-related space, arranged by time. (b) pattern in the evaporation-related space, orgnized by cumulative potential evapotranspiration (CET$_0$).
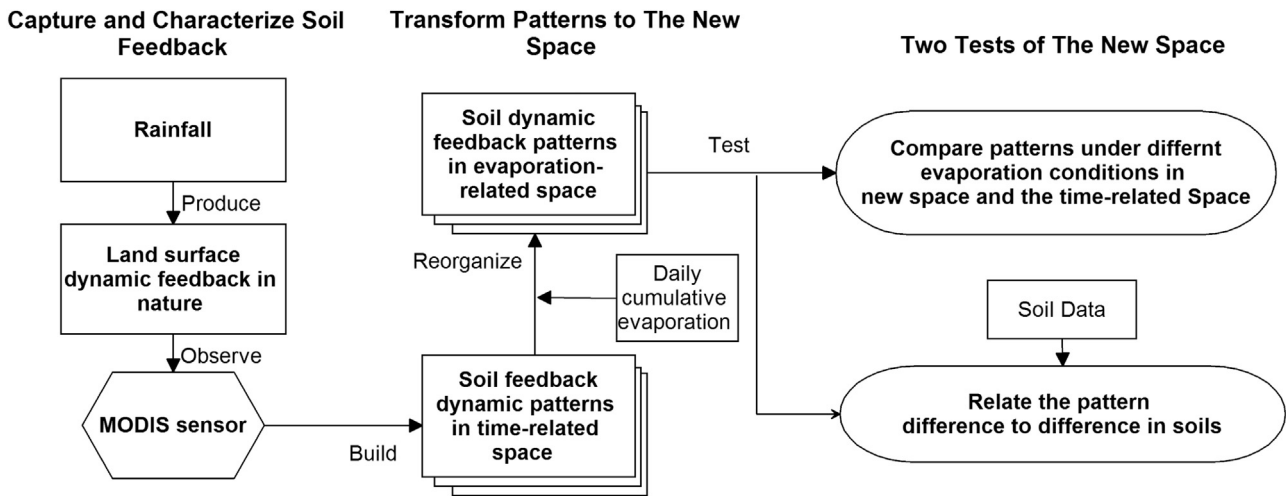
Fig. 2. Two stages transform the pattern from time-related space to evaporation-related space and test the reliability of the new space.

will have a similar curve at every step of soil evaporation. In other words, the same soil will have similar soil surface reflectance at every level of evaporation. The patterns for the same soil in different rain events should thus be similar in evaporation-related space, but it could be different in time-related space since the evaporations of two different locations in each time steps are not necessarily the same. To make it possible to compare patterns from different evaporation conditions is therefore to transform patterns from the original time-related space into the new evaporation-related space, specifically by finding an appropriate evaporation variable to serve as a new X axis, replacing time in the original space. Then, in this new space, the soil feedback pattern after a rainfall shows the fluctuation of soil surface reflectance with continued soil evaporation.

To distinguish the new space from the original space, we named the new space "the evaporation-related space" and the original space, which was first introduced by Zhu et al. (2010a) as "the time-related space." Fig. 1a and b shows an example of the same soil surface data from one rain event at a given location displayed in the time-related space and the evaporation-related space.

2.2. Methods

There are two steps to making the patterns for different evaporation conditions comparable (Fig. 2). The first step is to capture and characterize soil feedback. In this step, after every rain event, daily soil surface reflectance was captured and characterized by the MODIS sensor. The soil feedback patterns were organized by rain event and arranged in original time-related space. In the second step, the time-related patterns at each location were transformed to the evaporation-related space by calculating the cumulative potential evapotranspiration (CET_0) for each day after the rain.

Before applying the evaporation-related space in practice, we needed to validate this new space and compare it to the original. For the validation, two different tests were implemented in order to check: 1) whether the evaporation-related space was better at measuring spectral reflectance under different evaporation conditions compared to the time-related space; and 2) whether the differences in the patterns in the evaporation-related space still relate to the differences in the soils.

2.2.1. Capture and characterize soil feedback

To capture and characterize soil feedback after rainfall, high temporal resolution satellite data is needed. USGS MODIS daily surface reflectance data (MOD09) in Terra from 2000 to 2011 were used in this study (http://earthexplorer.usgs.gov/). The observation

window for each year was from April to May. During these months, the entire study area has no snow cover and has not fully started the planting season. In this observation window, few crop residues were left in the field. Most of them either have been removed by famers before planting, or have decomposed in soil after long time covered by snow during winter season. The low vegetation cover of farmland during this period allows the satellite sensor to obtain bare soil surface reflectance. Images for the seven days immediately following precipitation were collected to capture the soil drying processes. Bands 1–7 of MODIS data, which demonstrate the surface reflectance of shortwave radiation from the visible and near-infrared (VNIR: 400–1100 nm) to short wave infrared region (SWIR: 1100–2500 nm) of the electromagnetic spectrum, were used to build the feedback pattern.

To distinguish different rain events, the NASA Daymet dataset (http://daymet.ornl.gov/) was used as the input meteorological data, which provides gridded estimates of daily weather parameters, including daily highest and lowest air temperature, and precipitation(Thornton et al., 2014). The spatial resolution of air temperature and precipitation is $1\,km \times 1\,km$. Considering the strong spatial continuity of precipitation and temperature data, 1 km spatial resolution is suitable to match MODIS data and soil map in this study, which have 250 m spatial resolution. Rain events with more than 0.5 in. (12.7 mm) of precipitation were considered as valid rain events that could provide a sufficient amount of water to ensure a saturated surface layer in the soil at the initial stage of soil evaporation. The 0.5-in. limit was chosen according to precipitation and soil moisture observations in the SCAN weather station in Mason County, Illinois. (http://www.wcc.nrcs.usda.gov/scan/).

In data preprocessing, reflectance data from all bands were resampled to 250 m pixel size to utilize the spatially detailed spectral data from the red and NIR1 bands. In addition, NASA's cloud mask product (MOD35) was used to remove cloud cover in the image (Data Source: http://ladsweb.nascom.nasa.gov/data/search.html). Data selection, based on a series of bounding thresholds, ensured that the data used to build the soil feedback pattern were not influenced by the open water, thin clouds and partial vegetation cover. For example, the reasonable bare soil data bounds for MODIS Band1 (459–479 nm) values were set to 0.03–0.0625, which can remove the cumulative water effect and thin cloud effect (Lobell and Asner, 2002; Platnick et al., 2003; Fabre et al., 2015). Areas with a NDVI less than 0.3 were considered bare land or contained very sparse vegetation coverage (Liu et al., 2012).

2.2.2. Transform patterns to the new space

Cumulated potential evapotranspiration (CET_0) was used as the evaporation variable to reorganize soil surface reflectance after different rain events. CET_0 was chosen to represent soil evaporation because it is highly related to cumulative bare soil evaporation CE_s in the soil evaporation process (Gallardo et al., 1996; Ventura et al., 2006). Specifically, in the initial stage, soil evaporation (CEs) is equal to potential evaporation since there is enough water that can freely evaporate from the soil's top layer. As the surface dries, soil evaporation goes into a second stage. In this stage, the evaporation process is limited by the amount of water that can be transferred from deeper soil layers to the top layer. Previous studies have shown a linear relationship between CEs and the square root of CET_0 in the second stage (Ritchie, 1972; Stroosnijder, 1987). CET_0 can also be easily measured over a large area from daily weather observations, such as daily temperature and water vapor pressure, using the Penman-Monteith equation (Allen, 1998) or other experiential equations(Martínez-Cob and Tejero-Juste, 2004). The cumulative process starts on the first day after the rain event and continues to the day soil reflectance measured by the satellite sensor by summing up the daily ET_0 after the rain event Eq. (2).

The Hargreaves reference evapotranspiration equation (1985) was used to calculate daily potential evapotranspiration based on daily maximum and minimum air temperature data(Martínez-Cob et al., 2004). This equation has acceptable accuracy for obtaining the potential evapotranspiration in mid-arid areas and requires few weather parameters (Allen, 1998). In this equation, the only required observation is daily temperature, which is a basic weather observation variable and is available in most areas. The wide availability of the data makes the method simple to apply over a large area.

$$ET_0 = 0.0023 \times (T_{mean} + 17.8) \times (T_{max} - T_{min})^{0.5} \times R_a \qquad (1)$$

$$CET_{0j} = \sum_{i=1}^{j} ET_{0i} \qquad (2)$$

where is the reference evapotranspiration (potential evapotranspiration); CET_{0j} is cumulative ET_0 potential evapotranspiration j days after the rain event. T_{mean} is equal to $T_{max} - T_{min}/2$; R_a is extraterrestrial radiation for daily periods, which can be calculated by a given latitude and date, based on the equation given by the FAO56 document.

The more accurate estimation of daily ET_0 will certainly describe the real soil evaporation better during the soil drying process. According to the FAO56 document, the 1985 Hargreaves equation can be verified in each new region by comparing it with estimates from the FAO Penman–Monteith equation at weather stations where solar radiation, air temperature, humidity, and wind speed are measured. For each location, the Hargreaves equation error better reveals the linear stability bias. If necessary, the Hargreaves equation can be calibrated on a monthly or annual basis by determining empirical coefficients where ET_0 (Penman–Monteith equation)= $a + b$ ET_0 (1985 Hargreaves equation) (Allen, 1998). The coefficients a and b can be determined by regression analyses.

After calculating the daily cumulative potential evapotranspiration for each day after a rain event, patterns from original time-related space can be transformed to the evaporation-related new space by changing the X axis to the cumulative potential evapotranspiration (CET_0).

2.2.3. Evaluation

Two tests are necessary before patterns in evaporation-related space can be used as environmental covariates to indicate the spatial variation of soils.

2.2.3.1. Compare the evaporation-related space with the time-related space.

The objective of the first test is to test whether the evaporation-related space performs better at managing soil reflectance in different evaporation conditions. Specifically, the test determines whether the collected soil surface reflectance from the same soil but under different evaporation conditions has similar patterns in evaporation-related space. As mentioned before, the soil feedback pattern is influenced by both evaporation conditions and soil characteristics. In order to test the ability of the new space to manage soil reflectance in different evaporation conditions, the soil type must be controlled. Therefore, soil surface reflectance data at a given location after multiple rain events were collected as test data since during different rain events, the soil remains the same but evaporation conditions vary.

In order to compare the evaporation-related space to the time-related space, the same regression model was used to fit the same data set in both spaces. This comparison was independently applied to every location in the entire study area. The reflectance data from multiple rain events under different evaporation conditions was expected to be more closely distributed in the evaporation-related space and to be easily represented by the same regression surface. To best fit the nonlinear relationship in both spaces, a polynomial regression was applied separately to each band. In both spaces, a 3rd-order polynomial regression was considered acceptable for capturing the nonlinear relationship between time and soil reflectance in time-related space and CET0 and soil reflectance in evaporation-related space.

The root mean square error (RMSE) was used as a quantitative measurement to describe how data from different evaporation conditions scattered in both spaces. A lower RMSE indicates data with different evaporation conditions in that space more tends to present the same regression surface. A higher RMSE indicates that the variation of soil surface reflectance can hardly be described by the corresponding regression model. In other words, patterns with different evaporation conditions are more distributed away from the regression line when RMSE is high. The lower the RMSE, the closer the data points are to the regression line. RMSE was estimated by:

$$RMSE = \sqrt{\frac{\sum_{i=1}^{n}(P_i - O_i)^2}{n}} \qquad (3)$$

where P_i is the predicted soil surface reflectance by regression model on day i. O_i is the observed value of soil surface reflectance on day i. n is the number of data size.

The difference between the RMSE in the evaporation-related space and the time-related space is described as the RMSE difference.

$$\triangle RMSE = RMSE_{evaporation} - RMSE_{time} \qquad (4)$$

To calculate $\triangle RMSE$, we use the same regression model to fit the same data in two different pattern space. $RMSE_{evaporation}$ represents the RMSE in evaporation-related space. $RMSE_{time}$ represents the RMSE in time-related space. When $\triangle RMSE$ is less than zero, the RMSE in the evaporation-related space is lower than the RMSE in the time-related space, which means data in the evaporation-related space are closer to the regression line. Considering data are from multiple rain events with different evaporation conditions. The negative $\triangle RMSE$ means the data in evaporation-related space can be fit most easily comparing to data in the time-related space. The smaller $\triangle RMSE$ blow zero, the more stable soil feedback pattern will be shown in the evaporation-related space. When $\triangle RMSE$ is greater than zero means there is little benefit in transforming data from the time-related to the evaporation-related space. Noticed that the lower RMSE often shows when the model over fit the data.
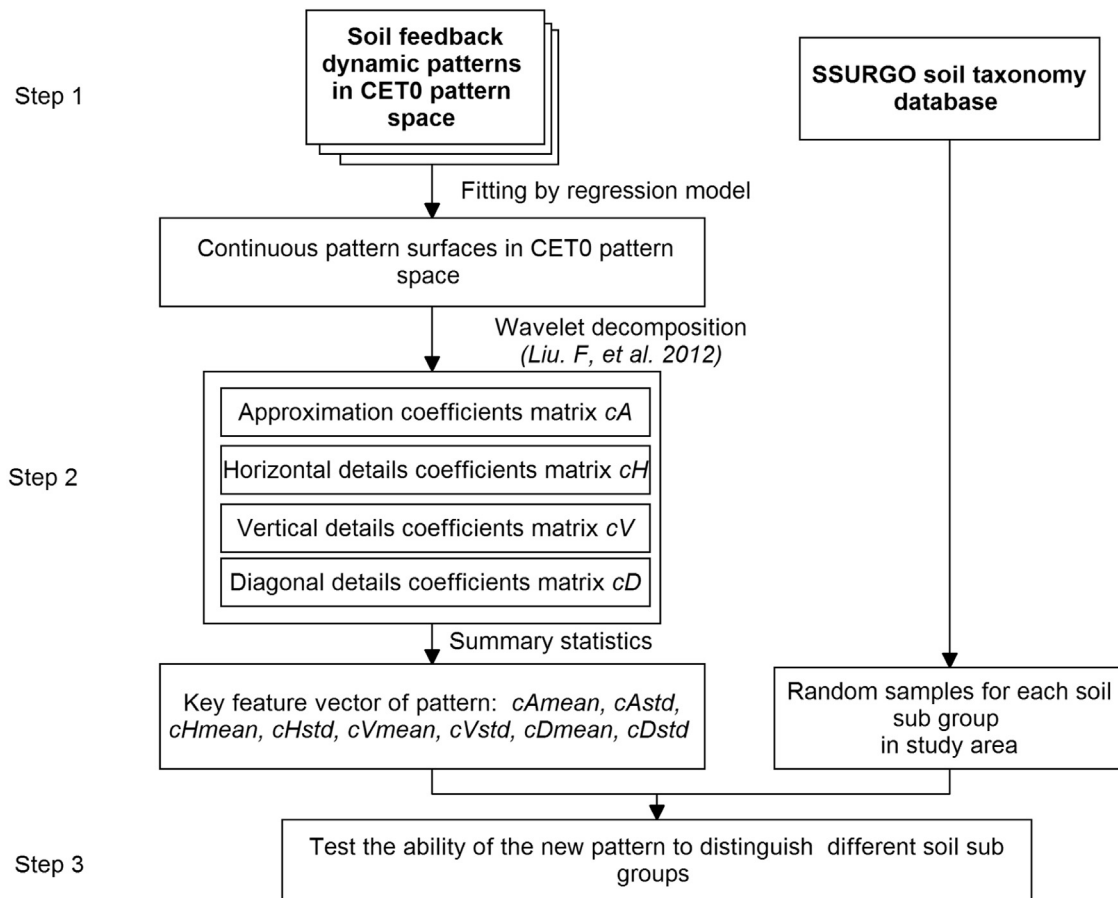
Fig. 3. Workflow for relating pattern differences to soil differences.

Therefore, the measurement of $\triangle$RMSE could also be influenced by over fit issues.

2.2.3.2. Relate pattern difference to the difference in soils. In previous studies, it has been shown that time-related pattern space can be used to distinguish different soils (Liu et al., 2012; Zhu et al., 2010a). The objective of the second test is to examine whether the difference in the soil feedback pattern in the evaporation-related space still can be related to differences in soil. The data processing method was based on the method introduced by previous research presented by Liu et al. (2012) with time-related pattern in south-central Manitoba, Canada. *T*-test was used to tell whether the patterns from different soil types are significantly different. The workflow is shown in Fig. 3 with three major steps.

In order to obtain the trend of soil surface reflectance changes during soil drying process and avoid the noise caused by different observation conditions, data in the evaporation-related space needs to be fitted with an appropriate regression model at each location to generate a continuous surface pattern to avoid noise caused by observation uncertainty. The fitting will also make it easier to compare the patterns at different locations. An exponential regression model was used to fit the relationship between soil reflectance in each band and the square root of daily cumulated reference evapotranspiration, $\sqrt{\mathrm{CET}_0}$. This model was derived from the equations used in soil evaporation studies and the relationship between soil surface reflectance and soil water content found in previous studies (Muller and Decamps, 2001; Ventura et al., 2006). The details of derivation have been shown in our previous study (Guo et al., 2015). After surface fitting, the soil feedback pattern at a given location can be described by serval equations, and the con-

tinuous soil feedback pattern for that location can be predicted by using these equations.

In order to more easily compare patterns from different locations, the second step, we extracted standardized feature vectors from each continuous pattern surface. The key features of a given pattern were described by four coefficient matrices calculated by a 2-D wavelet transformation of the pattern (Liu et al., 2012). The mean and standard deviations of each coefficient matrix were used to describe the key image texture from different directions. Specifically, the coefficient matrices include the approximation coefficients matrix (cA), horizontal detail coefficients matrix (cH), vertical detail coefficients matrix (cV), and diagonal detail coefficients matrix (cD). Ultimately, each pattern at a given location is represented by a feature vector {cAmean, cAstd, cHmean, cHstd, cVmean, cVstd, cDmean, cDstd}. Because each features have different variation and range, to make the comparison easier, each element of this feature vector over the study area is standardized to a range from 0 to 1.

With the feature vectors extracted from patterns, in the third step, we tested whether these feature vectors could be used to distinguish soil types. The Soil Survey Geographic Database (SSURGO) is used as the validation set in this study. SSURGO is a polygon-based database that contains soil types and soil properties collected in the USDA's National Cooperative Soil Survey(Soil Survey Staff b, 2014). Soil subgroup level taxonomy information was used to distinguish different soil types. Additionally, typical soil subgroup descriptions from the USDA were also used to describe the characteristics of the top-soil layer of each subgroup (https://soilseries.sc. egov.usda.gov).
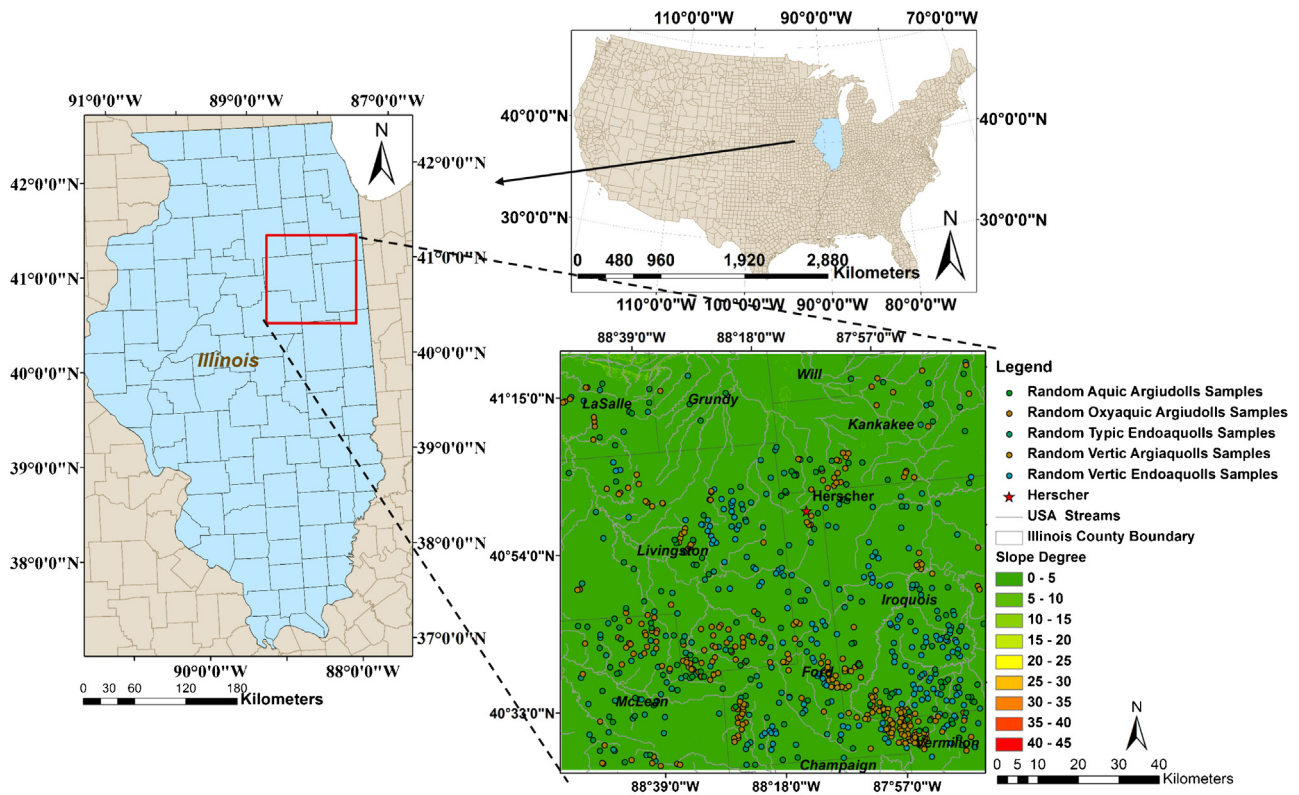
Fig. 4. Location of northeastern Illinois study area and spatial distribution of random soil samples for each soil subgroup from SSURGO database.

In each subgroup, 120 random locations were selected to represent that soil type. The sample points that fell into an area with a low R-square of exponential regression model were masked out, because observation data at these locations were not sufficient to capture the continuous soil feedback pattern. The mean value and 95% confidence interval of samples in each soil subgroup were calculated and compared with the other soil types. A T-test was used to test whether patterns from any two soil types were significantly different from each other. In addition, the Euclidean distance was also calculated between each soil subgroup pair, and was used as a quantitative variable to compare the difference between feature vectors of patterns in different soil subgroups. The Euclidean distance of two different soil types can be calculated by:

$$\text{Euclidean distance (soil1, soil2)} = \sqrt{\sum_{i=1}^{8} \left(V_{i(\text{soil1})} - V_{i(\text{soil2})} \right)^2} \quad (5)$$

where V_i is each feature of feature vector. The larger distance means the more difference between two soil feedback patterns. The smaller distance means that the patterns from these two soil types are more similar. After extracting key features from each soil feedback pattern by using the 2-D wavelet transformation, the ranges for each key feature in whole study area are different. Without standardization, Euclidean distance will be biased by the features which have large range or large values. The standardization process in the second step enhance the Euclidean distance to make it more sensitive to each difference between two soil feedback patterns in each feature.

3. Study area

A large, flat area of farmland (40.42° N-41.34° N and 87.73° W-88.94° W, about 10,000 km²) was selected as the study area in northeastern Illinois, in the United States (Fig. 4). According to the NOAA National Climatic Data Center weather data (1981–2010), the average precipitation for April and May in the study area is around 82 mm in April and 91 mm in May. Average temperatures are around 17 °C in April and 23 °C in May (NOAA, 2014). The entire area is part of the Ohio River basin which was influenced by Wisconsin glaciation events as a result of Pleistocene glaciation (Jacquemin and Pyron, 2011). The dominant parent materials of the soils are glacial till, glacial outwash, loess, lacustrine deposits and alluvium (Higgins, 1996). The major soil order in this area is Mollisol. According to the USDA Soil Survey Geographic Database (SSURGO) map, there are five major soil subgroups in this area, including Vertic Endoaquolls, Vertic Argiaquolls, Typic Endoaquolls, Oxyaquic Argiudolls and Aquic Argiudolls (Soil Survey Staff, 1999). As it is shown in Fig. 4, most part of study area is low-relief farmland. The average slope is 0.66°, with a standard deviation of 0.92. Elevation is in the range of 137–305 m, with a mean of 210 m, which is suitable for testing our research method. The major soil surface texture is silt loam, silty clay, silty clay loam. 120 random samples of each soil taxonomy type were collected from the SSURGO database in a subgroup level, which is shown in Fig. 4 by the different color points. These random samples were used in the second part of the test. Considering the MODIS sensor cannot directly observe soil surface reflectance in forested area, all these sampling points are located in bare soil area (farmland). The forested area and vegetated area were masked by a threshold of NDVI during data preprocessing.

4. Results and discussion

4.1. Comparison of evaporation-related space with time-related space

MODIS band 7, which is located in the short wave infrared region (SWIR: 1100–2500 nm), is most significantly influenced by changes to soil surface water content during the soil drying process. We
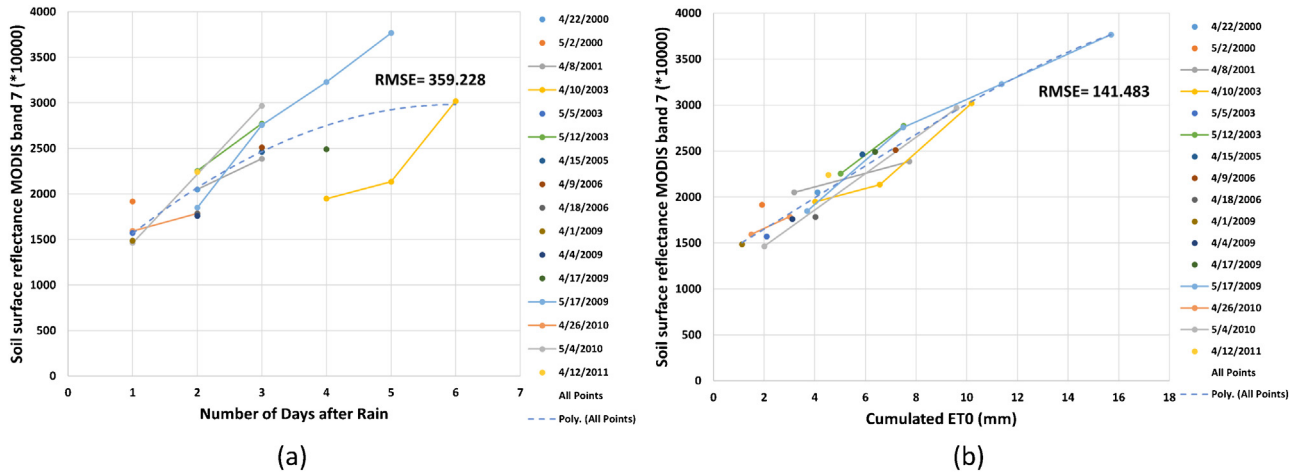
Fig. 5. Soil surface reflectance in MODIS band 7 variety during different rain events at a given location (87.871507 W, 40.491700 N) (a) Reflectance changes in time-related space. (b) Reflectance changes in new space. (For interpretation of the references to color in the text, the reader is referred to the web version of this article.)
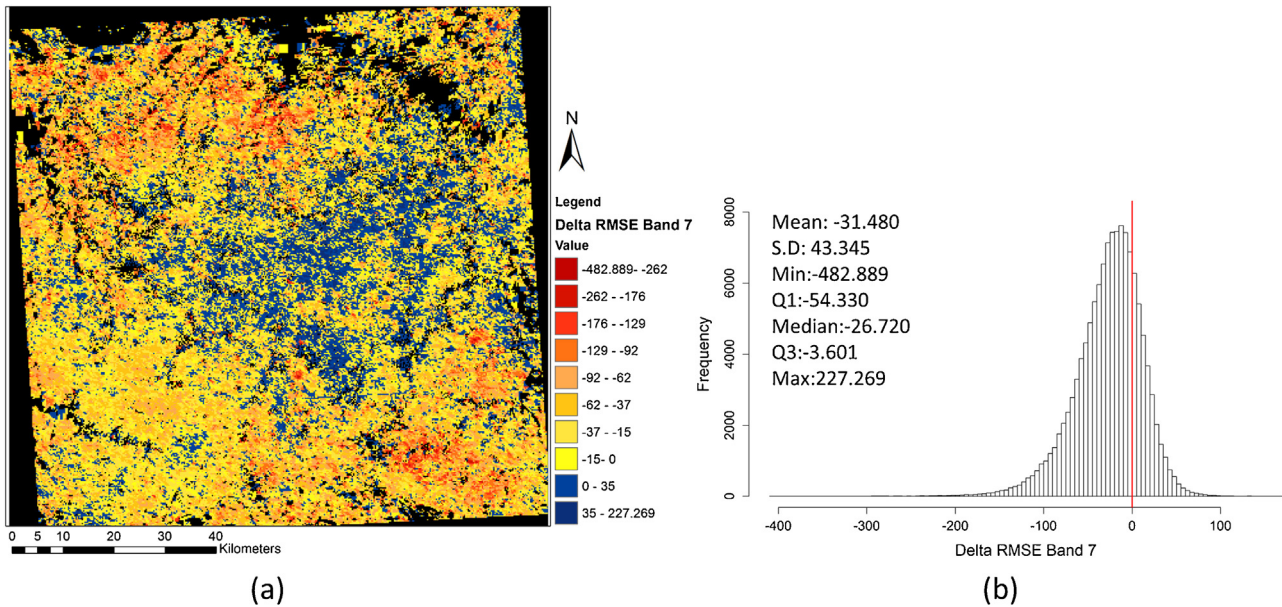

Fig. 6. Delta RMSE distribution of MODIS band 7 over the entire study area. (a) spatial distribution of Delta RMSE. (b) histogram of Delta RMSE. (For interpretation of the references to color in the text, the reader is referred to the web version of this article.)

Table 1
Statistical prameters of Delta RMSE from band1 to band7 in overall study area.

	Mean	S.D	Min	Q1	Median	Q3	Max
Band1	0.23	5.43	−60.64	−2.46	0.44	3.22	49.96
Band2	−0.94	8.72	−76.20	−5.29	−0.36	3.99	74.70
Band3	−0.43	13.30	−540.40	−6.06	0.23	6.08	225.60
Band4	−7.17	21.73	−457.40	−16.67	−5.16	4.14	290.60
Band5	−10.54	32.86	−772.50	−24.37	−8.09	5.63	787.80
Band6	−21.13	37.43	−461.00	−41.03	−18.70	1.23	246.10
Band7	−31.48	43.35	−482.89	−54.33	−26.72	−3.60	227.27

Number of pixels: 125,696.

therefore first focus our discussion on the dynamic changes in band 7 during the drying process, and discuss other bands later in this section.

We first compared dynamic changes in band 7 in two spaces at the pixel level. As shown in Fig. 5, at a given location (87.871507 W, 40.491700 N), soil surface reflectance in MODIS band 7 after multiple rain events appeared in both the time-related space (Fig. 5a)

and the evaporation-related space (Fig. 5b). The dot represents the data from just one day that is available after that rain event, such as data from 4/22/2000. The line represents 2–3 days of data that were available after a rain event, such as data from 4/10/2003. Different colors represent different rain events. The dashed line is the polynomial regression line. From Fig. 5(a), we can see that the soil reflectance on the 4/6/2003 rain event
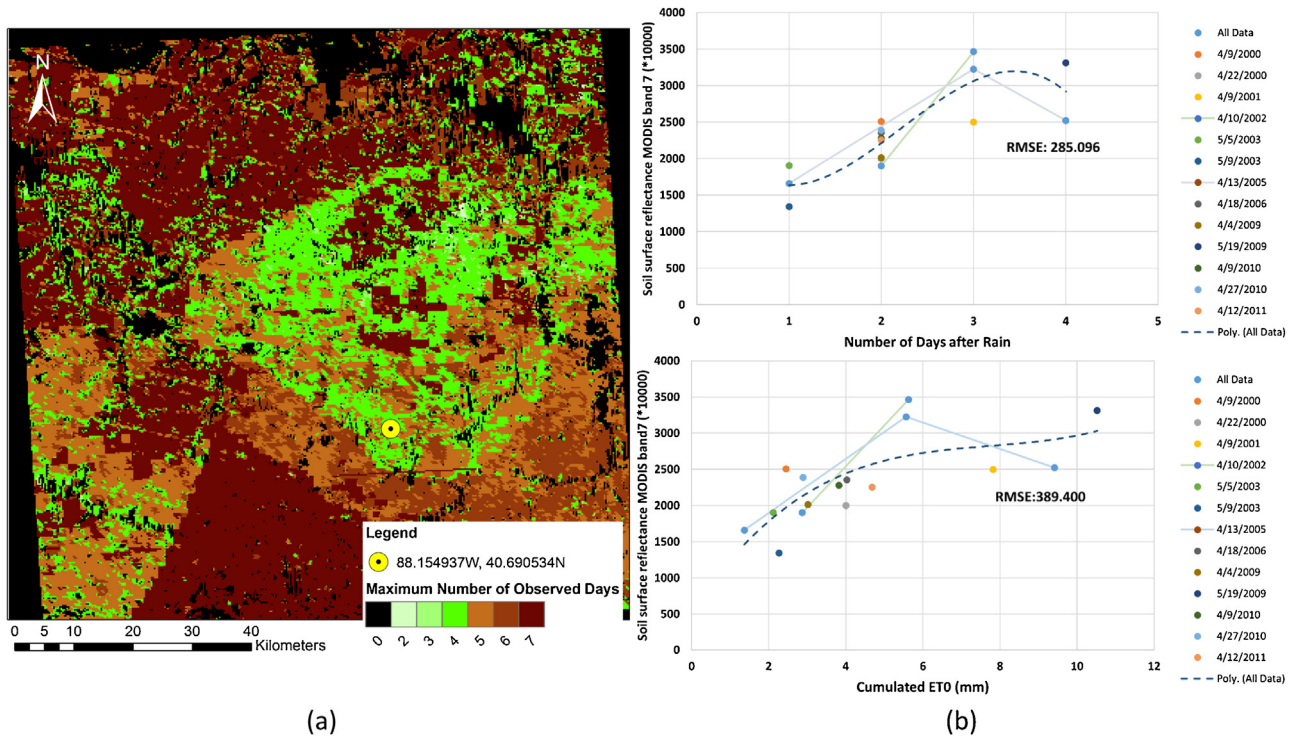
(a)   (b)

Fig. 7. Regression models tend to have an overfitting problem in the time-related space. (a) Maximum number of observed days after rain event over entire study area. (b) Soil reflectance data at a given location (88.154937 W, 40.69053 N) shown in two spaces, where in time-related space (above), the over fitted regression line shows lower RMSE compared to the same data in evaporation-related space (below). (For interpretation of the references to color in the text, the reader is referred to the web version of this article.)

Table 2
Typical soil series descriptions in top layer of soil in study area.

Soil Subgroups	Soil Great Group	Color	Surface Texture	Surface Structure
Aquic Argiudolls	*Argiudolls*	*Wet: black (10 YR 2/1); Dry: dark grayish brown (10YR 4/2)*	*silt loam*	*moderate fine granular structure; friable*
Oxyaquic Argiudolls	*Argiudolls*	*Wet: very dark gray (10 YR 3/1); Dry: gray (10 YR 5/1)*	*silt loam*	*moderate fine granular structure; friable*
Vertic Endoaquolls	*Endoaquolls*	*Wet: black (10 YR 2/1); Dry: dark gray (10 YR 4/1)*	*silty clay*	*weak very fine granular structure; friable; Cracks happen when dry*
Typic Endoaquolls	*Endoaquolls*	*Wet: black (10 YR 2/1); Dry: dark gray (10 YR 4/1)*	*silty clay loam*	*weak fine granular structure; firm*
Vertia Argiaquolls	*Argiaquolls*	*Wet: very dark gray (10 YR 3/1); Dry: gray (10 YR 5/1)*	*silt loam*	*weak thin platy structure parting to weak fine granular; friable, few fine continuous tubular pores; Cracks happen when dry*

Data. source: USDA official soil series descriptions (https://soilseries.sc.egov.usda.gov/osdquery.aspx).
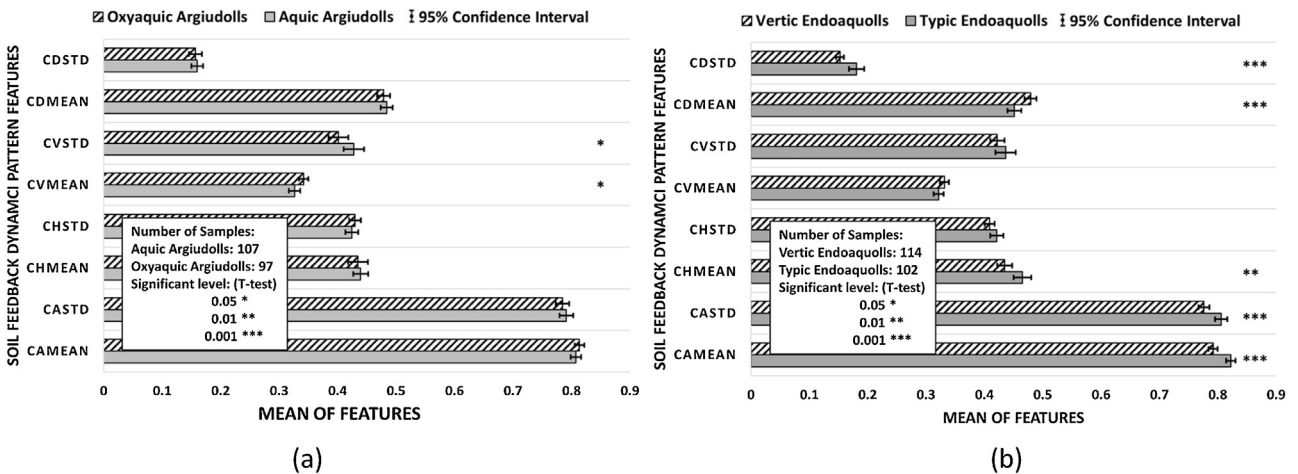

(a)   (b)

Fig. 8. Comparison of pattern features between two pairs of soils within the same great group. (a) Oxyaquic Argiudolls and Aquic Argiudolls. (b) Vertic Endoaquolls and Typic Endoaquolls.
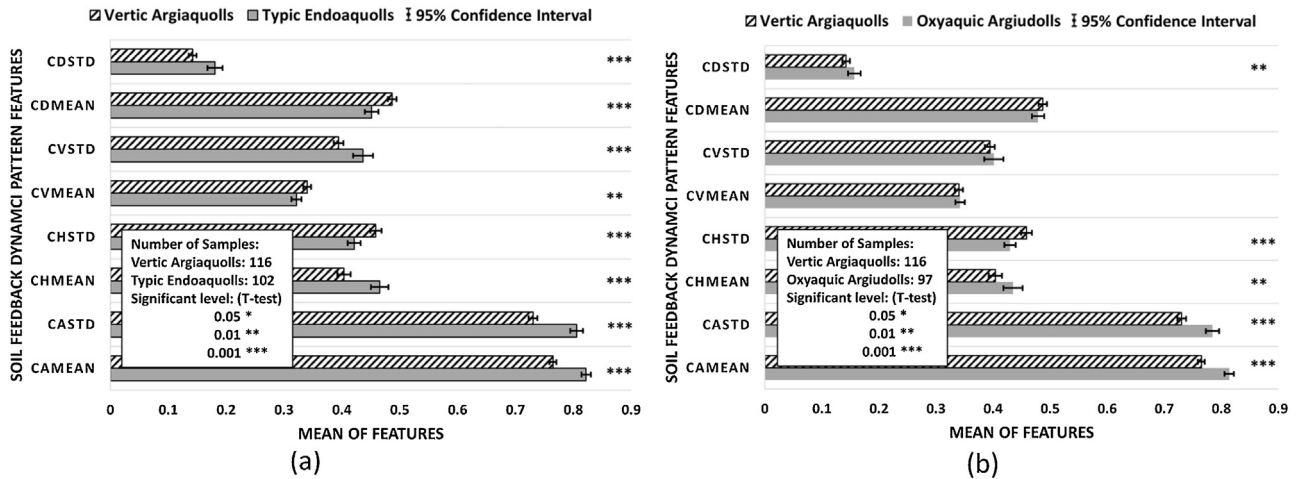
Fig. 9. Comparison of pattern features for two pairs of soils within different great grousp. (a) Vertic Argiaquolls and Typic Endoaquolls. (b) Vertic Argiaquolls and Oxyaquic Argiudolls.
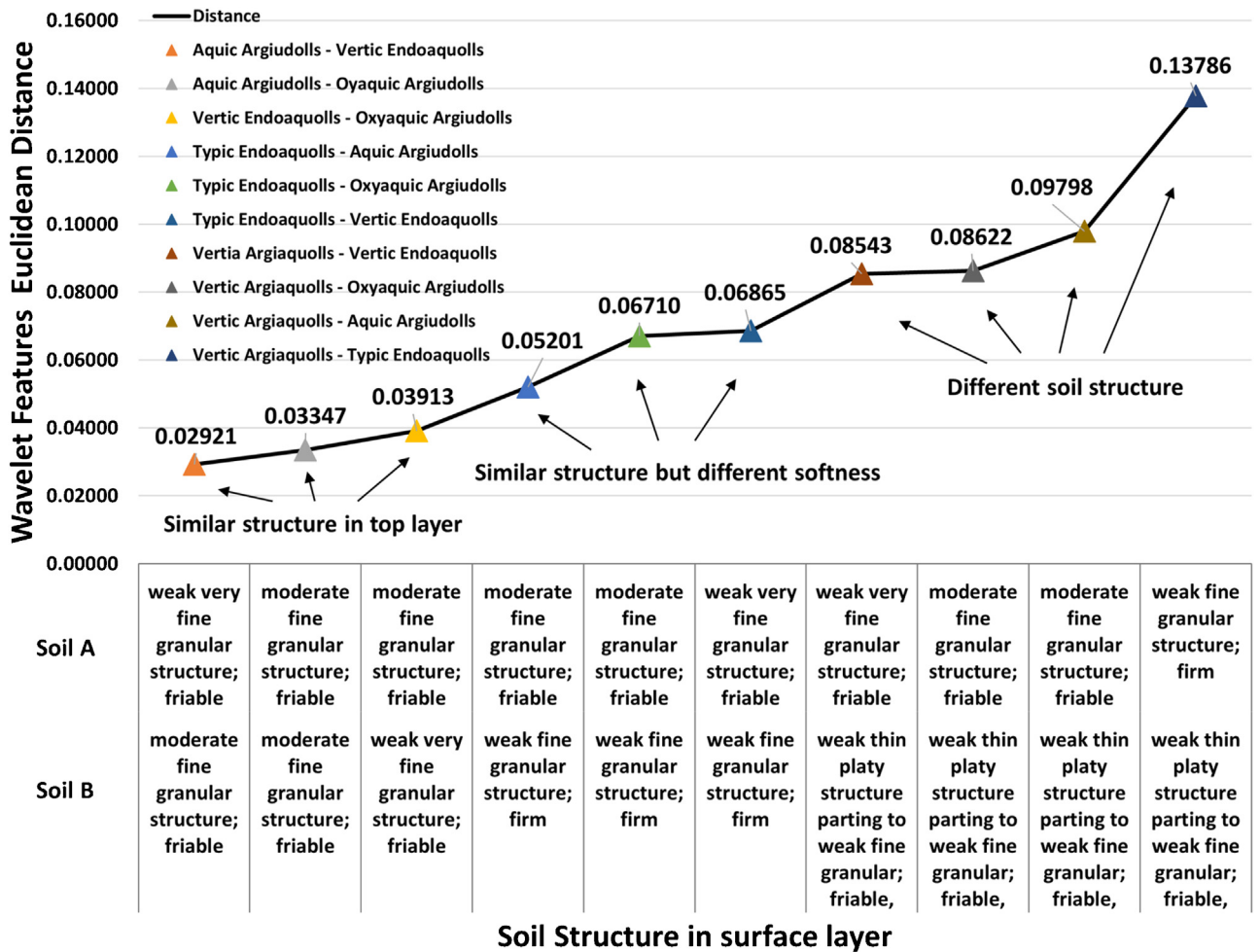

Fig. 10. Soil feedback pattern features Euclidean distance for each soil structure pair. (For interpretation of the references to color in the text, the reader is referred to the web version of this article.)

(the first observed data is on 4/10/2003) is significantly different from other rain events. This is because after this rain event, air temperatures were lower than usual, and daily evaporation was much lower than it would be with warmer temperatures. But encouraging results are shown in Fig. 5(b), where the same soil reflectance data was organized in the evaporation-related space.

Data from the 4/6/2003 rain event actually follows the same general pattern as the other rain events. The RMSE of the band7 prediction in the evaporation-related space is 141.483, which is much lower than the RMSE in the time-related space. Compared to the time-related space, this indicates that soil feedback patterns under different evaporation conditions are more likely to

follow the same uniform pattern in the evaporation-related space. And more importantly, this uniform pattern is not influenced by evaporation differences. In other words, the soil feedback patterns for different evaporation conditions can be compared over large areas.

Second, we compared two patterns at the regional level. For each location in the study area, the difference between the RMSE in the two spaces (delta RMSE) was calculated. As shown in Fig. 6(a), the delta RMSE was less than zero for most of the area (78.77%), which indicates that a uniform surface exists in the evaporation-related space when compared to the time-related space at most locations. A more reddish color indicates more negative delta RMSEs, which further suggests the advantage of using the evaporation-related space. Fig. 6(b) shows a histogram of delta RMSE for the entire study area. The red line represents the delta RMSE equal to 0. The negative delta RMSE is on the left of red line which is shown in yellow to red color in Fig. 6(a). The positive delta RMSE is on the right of red line which is shown in blue color in Fig. 6(a). The frequency distribution of delta RMSEs trends toward negative, which is indicated by a negative mean and negative median. The percentage of negative delta RMSE is 78.77%. This indicates that compared with the time-related pattern, soil surface reflectance under different evaporation conditions can be more easily fitted with a regression model in the evaporation-related space to get a more stable, uniform surface with lower RMSE in most of area.

In contrast, the blue color represents the positive values of delta RMSEs, which suggests that there was no improvement when using the evaporation-related space to organize soil surface reflectance. The blue area shown in Fig. 6(a) covers about 21.23% of study area. One possible reason for the presence of blue area in Fig. 6(a) is that in this area, the maximum number of days that have soil surface reflectance data available after multiple rain events is relatively small. This could lead to the overfitting of the regression model in the time-related space. Fig. 7(a) shows the maximum number of days that have soil surface reflectance data available after rain events. For the locations in blue, the maximum number of days was less than five. This means that soil surface reflectance data are available for the first four days, at most, after rain events. The available data after the multiple rain events can thus capture the soil surface reflectance only from the first day to the fourth day in those green areas. Take one location as an example (88.154937 W, 40.69053 N). Soil surface reflectance in both spaces is shown in Fig. 7(b), above and below. Compare to the evaporation-related space (Fig. 7b-below), the information that independent variables can provide in the time-related space is less than that in the evaporation-related space. For example, in the time-related space (Fig. 7b-above), the possible value of the X-axis at this location is limited by collection {1, 2, 3, and 4}, compared to the infinite possible values of the X-axis in the evaporation-related space. As a result, the regression is more likely to have an overfitting problem in the time-related space with lower RMSE when evaporation conditions in multiple rain events are more similar. But the same data, when shown in the evaporation-related space are more rational, as the soil surface reflectance increases at the beginning when the surface of the soil is losing water in the few days following a rain event. Then reflectance tends to be flat when the soil surface is dry. In contrast, as shown in Fig. 7(b)-above, time-related space does not show this flat trend. Comparing Fig. 6(a) and Fig. 7(a), it appears that the evaporation-related space preforms better with a larger maximum number of days.

To compare the performance of the evaporation-related space in other bands, the statistical parameters of Delta RMSE in band 1 to band 7 for the entire study area are shown in Table 1. The mean of delta RMSE decreases from band 1 to band 7. This is because in the bands closer to the short wave infrared region

(SWIR: 1100–2500 nm), the reflectance changes are more directly influenced by soil surface water content. In other words, it is more heavily influenced by different evaporation conditions. The means are clear negative from band4 (−7.172) to band 7 (−31.48), indicating that the RMSEs of the patterns in the evaporation-related space are smaller than those in the time-related space. Soil surface reflectance in MODIS Band 1 to band 3 are more sensitive to atmosphere conditions and partially vegetated area. So soil water content change is no longer the major reason causing soil reflectance change in these bands. As it is shown in Table 1, the difference of RMSEs in both evaporation-related pattern space and the time-related pattern space is very small with the mean and median of delta RMSE both close to 0. Overall, this result confirms that the soil feedback pattern under different evaporation conditions tends to follow the same surface more often in the evaporation-related space with lower RMSE as measured by the regression model. This advantage becomes clearer for the bands that are more sensitive to evaporation conditions.

4.2. Relationship of pattern differences to differences in soils

According to the SSURGO soil database, there are five main soil subgroups in this study area. The official soil series descriptions of these five soil subgroups are shown in Table 2(USDA, 2014).

First, we compared the pattern of the soils that belong to the same soil great group but differ at the subgroup level. A T-test was applied to test whether the samples of two different soils have significant different mean values in terms of pattern features. In Fig. 8(a), soils Oxyaquic Argiudolls and Aquic Argiudolls are both from the same soil great group, Argiudolls, with the same soil surface texture and surface structure. These two soils are thus more similar in eight features of soil feedback patterns. Only *cVmean* and *cVstd* features have some difference at a 0.05 level of significance. Fig. 8 (b) shows the pattern differences between Vertic Endoaquolls and Typic Endoaquolls, two soils that are also from the Endoaquolls soil great group, but these two patterns show significant differences with *cAmean, cAstd, cDmean, cDstd* at a 0.001 level of significance. This is because these two soils differ significantly in surface texture and surface structure. According to the soil description, Vertic Endoaquolls, which has more clay content in the top layer, is more friable and can easily crack in the drying process. Considering soil texture and the structural control of water movement during the soil drying process, the difference in the soil feedback patterns may be related to soil surface texture and surface soil structures.

Second, we compared the patterns of soils from different great groups. When soils come from different great groups with different surface texture and surface soil structure, the difference in soil feedback patterns is more significant. Fig. 9 shows the considerable difference between Vertic Argiaquolls and other soils. According to the official soil series descriptions, the top layer soil structure of Vertic Argiaquolls is a weak, thin, platy structure with a weak, fine granular structure, and Vertic Argiaquolls also cracks when the soil becomes dry. Results show a significant difference between Vertic Argiaquolls and Typic Endoaquolls soils. Most of the eight pattern features, like *cAmean* and *cHmean,* have a difference at a 0.001 significance level (Fig. 9a). Similarly, Vertic Argiaquolls differ significantly compared to Oxyaquic Argiudolls in *cAmean, cAstd*, and *cHstd* at the 0.001 level (Fig. 9b).

On the other hand, our comparative analysis shows that the differences in the soil feedback pattern in the new space are highly related to soil surface differences in texture and structure. These findings align with the common-sense expectation that the more differences in soil structure, the more differences appear in the soil

drying process, and as a result, the more differences appear in the soil feedback patterns.

The Euclidean distance of each pair of soil feedback patterns was used to quantify the pattern difference for each soil subgroup pair (Fig. 10). The Euclidean distance of patterns were found to increase as the soil surface structure differences increase. There are two soils that differ significantly from others, Typic Endoaquolls and Vertic Argiaquolls. Based on USDA official soil series descriptions, Typic Endoaquolls is more compacted than other soils, and Vertic Argiaquolls contains thin, platy structures and tubular pores that could significantly influence the movement of water in the top layer of the soil during the drying process. This shows that the pattern differences between these two soils and other soils are significant. The results also indicate that the differences between patterns in the evaporation-related space are more related to soil structure and soil surface texture variation. It should be acknowledged that soils with similar surface structures are more likely to present similar patterns, even when they are not necessarily from the same taxonomy class.

5. Conclusions

In this study, we presented a new space for understanding soil feedback patterns in order to solve two problems of patterns in original time-related space. First, two patterns from different locations with unequal daily evaporation cannot be compared to each other; second, at a given location, the variation in evaporation conditions after different rain events led to considerable fluctuation in patterns, which makes patterns from different rain events impossible to compare. The new space, the evaporation-related space, was introduced to solve these two problems. The advantage of the evaporation-related space is that data can be collected from multiple rain events regardless of the variation in evaporation conditions. Two tests evaluated whether the evaporation-related space: 1) can better deal with patterns from different evaporation conditions than the original time-related space; and 2) is capable of characterizing most of the variation of soil subgroups over a large study area.

The case study in the northeastern Illinois suggests that, compared to the time-related space, soil surface reflectance from different rain events is more likely to present the same regression surface in evaporation-related space. Additionally, our comparative analysis in the second test shows that the differences in soil feedback patterns in the evaporation-related space are capable of distinguishing the different types of soil. Patterns in the evaporation-related space can also be used as environmental covariates to represent spatial variation of soil in flat areas. Furthermore, the result also indicates that the greater the difference in soil structures in the top layer, the more significant the difference in soil feedback patterns.

The findings are encouraging. The new space is an easy way to remove the influence of different evaporation conditions on the soil feedback pattern, and is easier to implement in digital soil mapping over large areas. The methodology provides a new way to organize and construct a soil feedback pattern based on historical soil reflectance data after multiple rain events, and it overcomes the limitation that the time-related soil feedback dynamic pattern must be built in the same rain event.

The specific practical application of this study will be the digital soil mapping. After solving the comparable problems of patterns in different evaporation conditions, soil feedback pattern can be used to describe the spatial variation of soil in large low relief areas. A further study will focus on what soil properties can be represented by this new data source and what level of accuracy can be obtained to predict spatial variation in soil by using the new soil feedback pattern combined with other traditional environmental covariates (such as topographic information).

References

Allen, R.G., 1998. FAO Irrigation and drainage paper No. 56. Irrig. Drain 300, 64–65.
Anderson, K., Croft, H., 2009. Remote sensing of soil surface properties. Prog. Phys. Geogr. 33, 457–473.
Coleman, T.L., a, Agbu P., Montgomery, O.L., 1993. Spectral differentiation of surface soils and soil properties; is it possible from space platforms. Soil Sci. 115, 283–293.
Fabre, S., Briottet, X., Lesaignoux, A., 2015. Estimation of soil moisture content from the spectral reflectance of bare soils in the 0.4–2.5 μm domain. Sensors 15, 3262–3281, http://dx.doi.org/10.3390/s150203262.
Gallardo, M., Snyder, R., Schulbach, K., Jackson, L., 1996. Crop growth and water use model for lettuce. J. Irrig. Drain. Eng. 122, 354–359.
Gomez, C., Lagacherie, P., Coulouma, G., 2008. Continuum removal versus PLSR method for clay and calcium carbonate content estimation from laboratory and airborne hyperspectral measurements. Geoderma 148, 141–148, http://dx.doi.org/10.1016/j.geoderma.2008.09.016.
Guo, S., Meng, L., Zhu, A.-X., Burt, J., Du, F., Liu, J., Zhang, G., 2015. Data-gap filling to understand the dynamic feedback pattern of soil. Remote Sens. 7, 11801–11820, http://dx.doi.org/10.3390/rs70911801.
Higgins, S., 1996. USDA Soil survey of livingston county, Illinois [WWW Document]. URL http://www.nrcs.usda.gov/wps/portal/nrcs/surveylist/soils/survey/state/?stateId=IL (accessed 26. 05. 14.).
Iqbal, J., Thomasson, J.A., Jenkins, J.N., Owens, P.R., Whisler, F.D., 2005. Spatial variability analysis of soil physical properties of alluvial soils. Soil Sci. Soc. Am. J. 69, 1–13, http://dx.doi.org/10.2136/sssaj2004.0154.
Jacquemin, S.J., Pyron, M., 2011. Impacts of past glaciation events on contemporary fish assemblages of the Ohio river basin. J. Biogeogr. 38, 982–991, http://dx.doi.org/10.1111/j.1365-2699.2010.02457.x.
Jenny, H., 1941. Factors of soil formation. In: A System of Quantitative Pedology. McGraw-Hill, New York.
Lagacherie, P., Baret, F., Feret, J.B., Madeira Netto, J., Robbez-Masson, J.M., 2008. Estimation of soil clay and calcium carbonate using laboratory, field and airborne hyperspectral measurements. Remote Sens. Environ. 112, 825–835, http://dx.doi.org/10.1016/j.rse.2007.06.014.
Lal, R., Shukla, M.K., 2004. Principles of Soil Physics. Marcel Dekker, New York.
Liu, F., Geng, X., Zhu, A.-X., Fraser, W., Waddell, A., 2012. Soil texture mapping over low relief areas using land surface feedback dynamic patterns extracted from MODIS. Geoderma 171–172, 44–52, http://dx.doi.org/10.1016/j.geoderma.2011.05.007.
Lobell, D.B., Asner, G.P., 2002. Moisture effects on soil reflectance. Soil Sci. Soc. Am. J. 66, 722–727, http://dx.doi.org/10.2136/sssaj2002.0722.
Martínez-Cob, A., Tejero-Juste, M., 2004. A wind-based qualitative calibration of the Hargreaves ET0 estimation equation in semiarid regions. Agric. Water Manag. 64, 251–264, http://dx.doi.org/10.1016/S0378-3774(03)00199-9.
McKenzie, N., Ryan, P.J., 1999. Spatial prediction of soil properties using environmental correlation. Geoderma 89, 67–94, http://dx.doi.org/10.1016/S0016-7061(98)00137-2.
Mellouli, H., van Wesemael, B., Poesen, J., Hartmann, R., 2000. Evaporation losses from bare soils as influenced by cultivation techniques in semi-arid regions. Agric. Water Manag. 42, 355–369, http://dx.doi.org/10.1016/S0378-3774(99) 00040-2.
Mulder, V.L., de Bruin, S., Schaepman, M.E., Mayr, T.R., 2011. The use of remote sensing in soil and terrain mapping—a review. Geoderma 162, 1–19, http://dx.doi.org/10.1016/j.geoderma.2010.12.018.
Muller, E., Decamps, H., 2001. Modeling soil moisture−reflectance. Remote Sens. Environ. 76, 173–180.

NOAA, 2014. National Climatic Data Center weather data (1981–2010). [WWW Document] URL http://www.ncdc.noaa.gov/cdo-web/datatools/normals (accessed 16.05.14.).

Odeh, I.O.A., Mcbratney, A.B., 2000. Using AVHRR images for spatial prediction of clay content in the lower Namoi Valley of eastern Australia. Geoderma 97, 237–254.

Philpot, W.D., 2010. Spectral reflectance of wetted soils. Art, Science and Applications of Reflectance Spectroscopy (ASARS) Proceedings of ASD and IEEE GRS; Art, Science and Applications of Reflectance Spectroscopy Symposium, 1–11, http://dx.doi.org/10.13140/2.1.2306.0169, 11pp, Boulder, CO.

Platnick, S., King, M.D., Ackerman, S. a., Menzel, W.P., Baum, B. a., Riédi, J.C., Frey, R. a., 2003. The MODIS cloud products: algorithms and examples from terra. IEEE Trans. Geosci. Remote Sens. 41, 459–472, http://dx.doi.org/10.1109/TGRS.2002.808301.

Ritchie, J., 1972. Model for predicting evaporation from a row crop with incomplete cover. Water Resour. Res. 8, 1204–1213.

Soil Survey Staff, 1999. Soil taxonomy: a basic system of soil classification for making and interpreting soil surveys. In: U.S. Department of Agriculture Handbook, 2nd ed. Natural Resources Conservation Service, pp. 436.

Soil Survey Staff b, 2014. Natural resources conservation service, united states department of agriculture. Web Soil Survey [WWW Document]. URL http://websoilsurvey.nrcs.usda.gov/(accessed 1.1.14).

Somers, B., Gysels, V., Verstraeten, W.W., Delalieux, S., Coppin, P., 2010. Modelling moisture-induced soil reflectance changes in cultivated sandy soils: a case study in citrus orchards. Eur. J. Soil Sci. 61, 1091–1105, http://dx.doi.org/10.1111/j.1365-2389.2010.01305.x.

Stroosnijder, L., 1987. Soil evaporation: test of a practical approach under semi-arid conditions. Netherlands J. Agric. Sci. 35, 417–426.

Sullivan, D., Shaw, J., Rickman, D., 2005. Using IKONOS imagery to estimate surface soil property variability in two alabama physiographies. Soil Sci. Soc. Am. J. 69, 1789–1798, http://dx.doi.org/10.2136/sssaj2005.0071.

Thornton, P.E., Thornton, M.M., Mayer, B.W., Wilhelmi, N., Wei, Y., Devarakonda, R., Cook, R.B., 2014. Daymet: Daily Surface Weather Data on a 1-km Grid for North America, Version 2. Data set [WWW Document]. Oak Ridge Natl. Lab. Distrib. Act. Arch. Center, Oak Ridge, Tennessee, USA. URL http://daac.ornl.gov.

USDA, 2014. USDA official soil series descriptions [WWW Document]. URL https://soilseries.sc.egov.usda.gov/osdquery.aspx (accessed 11.4.14.).

Ventura, F., Snyder, R.L., Bali, K.M., 2006. Estimating evaporation from bare soil using soil moisture data. J. Irrig. Drain. Eng. 132, 153–158.

Wang, L., Qu, J.J., 2009. Satellite remote sensing applications for surface soil moisture monitoring: a review. Front. Earth Sci. China 3, 237–247, http://dx.doi.org/10.1007/s11707-009-0023-7.

Weidong, L., Baret, F., Xingfa, G., Qingxi, T., Lanfen, Z., Bing, Z., 2002. Relating soil surface moisture to reflectance. Remote Sens. Environ. 81, 238–246.

Zhu, A.X., 1997. A similarity model for representing soil spatial information. Geoderma 77, 217–242, http://dx.doi.org/10.1016/S0016-7061(97) 00023-2.

Zhu, A.X., Liu, F., Li, B., Pei, T., Qin, C., Liu, G., Wang, Y., Chen, Y., Ma, X., Qi, F., Zhou, C., 2010a. Differentiation of soil conditions over low relief areas using feedback dynamic patterns. Soil Sci. Soc. Am. J. 74, 861–869, http://dx.doi.org/10.2136/sssaj2008.0411.

Zhu, A.X., Yang, L., Li, B., Qin, C., Pei, T., Liu, B., 2010b. Construction of membership functions for predictive soil mapping under fuzzy logic. Geoderma 155, 164–174, http://dx.doi.org/10.1016/j.geoderma.2009.05.024.